Mathematical models and numerical simulations for electro-hydrostatic servo-actuators

Dinca Liviu, Corcau Jenica, Lungu Mihai, Tudosie Alexandru

***Abstract*—** The electro-hydrostatic servo-actuators are expected to be the future of the actuations of the aircraft command surfaces. This paper presents some problems concerning these actuators and two mathematical models. There are shown also the results obtained by numerical simulation using the mathematical models of the servo-actuator. One mathematical model uses volume flow ratios to describe the servo-actuator functioning and the other mass flow ratio.

***Keywords*—** aircraft command, hydraulic actuators, hydrostatic actuators, hydraulic systems.

I. Introduction

The hydraulic systems of big airliners reached some difficult problems along their exploitation. Some of these problems produced great aeronautic catastrophes and for this reason the idea to replace the centralized hydraulic system with small local hydraulic systems appeared.

One of the most difficult problems was the loosing of the hydraulic liquid. The hydraulic pipes sharing produce inevitably the loosing of the hydraulic liquid and in consequence the impossibility to command the aircraft. Although the hydraulic system is double or even triple redundant, in some cases, structure damages produced the hydraulic pipes sharing for all the hydraulic system. Even the structure damage permitted to continue the flight, the airplane crushed because the impossibility of command.

Another problem of the centralized hydraulic system is the energetic efficiency of the actuation. The classical actuators use hydraulic servo-valves as command device. In these servo-valves at least 30% of the hydraulic power is lost. Considering although the power lost on hydraulic pipes and the other equipments, the maximum efficiency of the centralized hydraulic system is about 30 – 40 % . A small local hydraulic system reduce the lost power and so the efficiency is improved.

A third problem is an economical one. The classical hydraulic systems needs high maintenance costs and long time to replace one fault equipment. This leads to long time of out of service for the aircraft. One small local hydraulic system may be built as one compact servo-actuator, easy to replace in a fault case.

Using such actuators some problems concerning the hydraulic systems are transferred to the electrical systems. The local hydraulic circuit has a small pump acted by an electrical motor. The entire power needed for the aerodynamic surface actuation is now supplied by the electrical system instead the hydraulic system. But the electrical power distribution is more reliable as the hydraulic power distribution. For a big commercial airplane, the power supplied by the electrical system may reach 1MW if such servo-actuators are used.

II. Hydraulic Schemes

Many hydraulic circuits were proposed to solve these problems. In fig. 1 is presented a solution with a gear pump driven by an electrical motor. The gear pump has constant speed. The command device is a hydraulic servo-valve. But the hydraulic servo-valve is expansive and the problem of hydraulic power lost in this device remains.

In fig. 2 the hydraulic servo-valve is replaced by a proportional distributor. The cost is smaller, but remains the problem of power lost in this device. The problem of dynamical qualities of the actuator is more difficult to solve in this case. The proportional distributor is sluggish than the servo-valve and the response time of the actuator increase considerably.

The optimum solution, developed by some producers is presented in fig. 3.

The pump supply direct the hydraulic cylinder, without another command device. Auxiliary elements such filters and valves are shown in fig. 3. A check valve is used to fix the hydraulic cylinder in the neutral position when the pump or the motor fault.

The hydraulic power lost only in short pipes, valves and filters is very small relative to the centralized hydraulic system provided with servo-valves. The efficiency of the hydraulic circuit in considerably improved.

The first part of this paper was presented at the conference WSEAS Venice, Italy, November 2008. It was revised and accepted for presentation. After the conference received the recommendation to be developed and published by NAUN Journal.

Dinca Liviu is lecturer at the University of Craiova, Romania, Faculty of Electrical Engineering, Department of Avionics. 107, Decebal Blvd., Craiova, Romania, ldinca@elth.ucv.ro .

Corcau Jenica is lecturer at the University of Craiova, Romania, Faculty of Electrical Engineering, Department of Avionics. 107, Decebal Blvd., Craiova, Romania, jcorcau@elth.ucv.ro.

Lungu Mihai is assistant at the University of Craiova, Romania, Faculty of Electrical Engineering, Department of Avionics. 107, Decebal Blvd., Craiova, Romania, mlungu@elth.ucv.ro.

Tudosie Alexandru is associate professor at the University of Craiova, Romania, Faculty of Electrical Engineering, Department of Avionics. 107, Decebal Blvd., Craiova, Romania, atudosie@elth.ucv.ro.

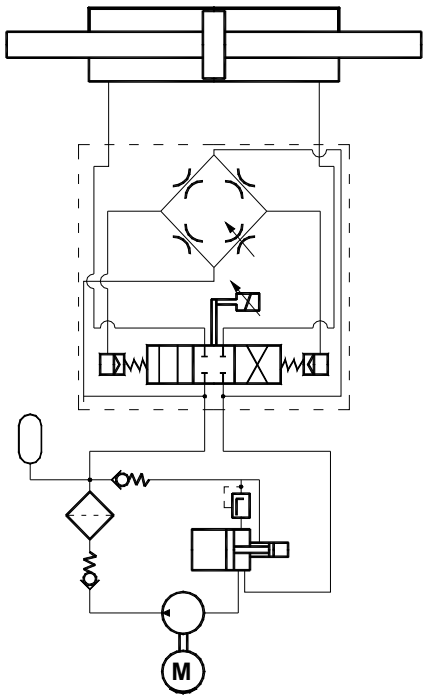

Fig. 1 Hydraulic local circuit with servo-valve

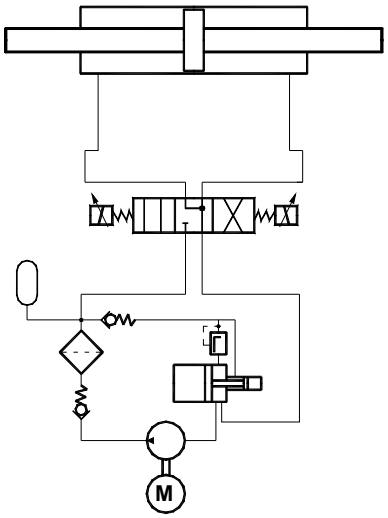

Fig. 2 Hydraulic local circuit with proportional distributor

The pump is a bidirectional gear pump and the command of the aerodynamic surface is obtained by the variation of the direction and the speed of the electric motor. The electric motor is a DC one and is provided with a controller which change the supply voltage accordingly the command received from the pilot.

One special problem is the hydraulic cylinder. Because the restrictive space on board it is not possible to use a bilateral rod cylinder. For this reason is used a special cylinder with one rod. This cylinder has the same effective area in the both movement directions [2].

In some variants the reservoir is replaced by a membrane hydro-accumulator which maintain the necessary pressure to the pump inlet. The hydro-accumulator is cheaper than the auto-pressurized reservoir and provide a sufficient quantity of hydraulic liquid.

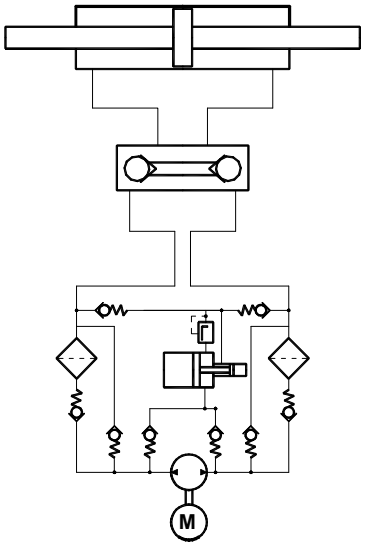

Fig. 3 Hydraulic local circuit driven by the motor speed

III. Mathematical Model With Volume Flow Ratio

This study describe the behavior of an electro-hydrostatic servo-actuator shown in fig. 3. A simplified scheme of the hydraulic circuit is presented in fig. 4.

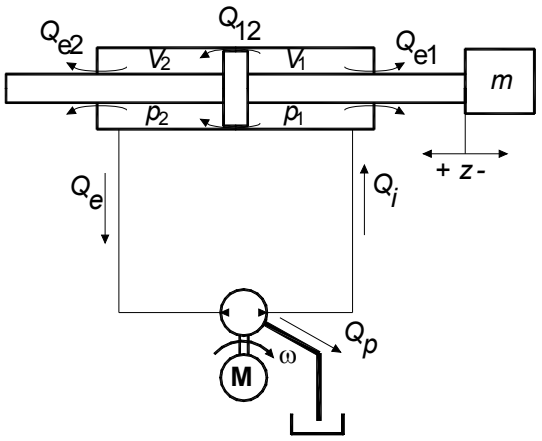

Fig. 4 Hydraulic circuit – simplified scheme

The flow rates through the pump and the leakage between the cylinder chambers, to the exterior and the leakage of the pump are taken to account. So, the equations which describe the hydraulic cylinder functioning are the following:

$$\beta\left(V_{01}+Sz\right)\frac{\mathrm{d}p_1}{\mathrm{d}t}=Q_1-Q_{e1}-Q_{12}-Q_{p1}-S\frac{\mathrm{d}z}{\mathrm{d}t}, \quad (1)$$

$$\beta\left(V_{02}-Sz\right)\frac{\mathrm{d}p_2}{\mathrm{d}t}=-Q_2-Q_{e1}+Q_{12}-Q_{p2}+S\frac{\mathrm{d}z}{\mathrm{d}t}. \quad (2)$$

$$Q_{12} = c_{12}(p_1 - p_2)\,,$$

$$Q_{e1} = c_1 p_1\,, \tag{4}$$

$$Q_{e2} = c_1 p_2\,, \tag{5}$$

$$Q_{p1} = c_2 p_1\,, \tag{6}$$

$$Q_{p2} = c_2 p_2\,, \tag{7}$$

$$Q_{pump} = D\omega\,, \tag{8}$$

$$m\frac{\mathrm{d}^2 z}{\mathrm{d}t^2} = (p_2 - p_1)S - f\frac{\mathrm{d}z}{\mathrm{d}t} - kz - F_u\,. \tag{9}$$

In (1) and (2) β is the compressibility coefficient of the hydraulic liquid and S is the piston section. In (8) D is the pump displacement and in (9) F_u is the dry friction force.

The linearization of these equations leads to

$$\frac{\mathrm{d}\Delta p_1}{\mathrm{d}t} = \left[-S\frac{\mathrm{d}z}{\mathrm{d}t} + D\omega - c_{12}(p_1 - p_2) - c_1 p_1 - c_2 p_1\right]\frac{1}{\beta V_1}, \tag{10}$$

$$\frac{\mathrm{d}\Delta p_2}{\mathrm{d}t} = \left[S\frac{\mathrm{d}z}{\mathrm{d}t} - D\omega + c_{12}(p_1 - p_2) - c_1 p_2 - c_2 p_2\right]\frac{1}{\beta V_2}. \tag{11}$$

If the movement is studied around the neutral point then $V_1 = V_2$ and from (10) and (11) we obtain

$$\frac{\mathrm{d}(\Delta p_1 - \Delta p_2)}{\mathrm{d}t} = \left[-2S\frac{\mathrm{d}z}{\mathrm{d}t} + 2D\omega - c_{tp}(p_1 - p_2)\right]\frac{1}{\beta V} \tag{12}$$

For the DC motor we considered the model

$$L\frac{\mathrm{d}i}{\mathrm{d}t} = -Ri - k_e\omega + U\,, \tag{13}$$

$$J\frac{\mathrm{d}\omega}{\mathrm{d}t} = k_t i - B\omega - M\,. \tag{14}$$

where

$$M = D\frac{1}{2\pi\eta_t}\Delta p\,. \tag{15}$$

We used the following notations: L - coil inductance, R - coil resistance, k_e - back-EMF constant, J - rotor momentum, k_t – torque constant, B – friction coefficient, M – resistant moment, η_t - total efficiency of the pump.

Using these equations a simulation scheme in SIMULINK was obtained.

For the control loop two variants of controller were studied. One classical proportional controller and one fuzzy controller. The input of the system is one voltage and the output is the movement of the aerodynamic surface. The control loop is closed through the reaction voltage received from the position transducer of the aerodynamic surface.

The DC motor controller receives the error signal, amplify it and feed the motor. For the DC motor feeding, the saturation phenomenon was taken into account.

For the fuzzy controller was chosen a Mamdani controller.

We chose seven linguistically terms for the error (input of the controller) and for the output. The error domain was considered from -50 to 50 and the output from -1 to 1. The membership functions for the fuzification process were considered triangular type, uniform distributed from -1 to 1. The extremely functions were considered trapezoidal type with the maximum at -1 and 1 and extended to the error value of -50 and 50. A number of 49 fuzzy rules were obtained. These rules were constructed on the principle of correspondence between input and output. The bisector method was considered for defuzification.

IV. Numerical Simulations -Volume Flow Ratio Model

The simulation schemes obtained in SIMULINK were used to study the servo-actuator behaviour in different conditions. In the simulations presented in this par of the paper the amplitude of the input signal was modified. The elastic constant k was kept, that means the aircraft speed was maintained constant.

The numerical values of the servo-actuator components parameters were obtained from technical specifications of the motor, pump and cylinder.

Parameters of actuated element:	
- mass m	20 kg
- viscous friction coefficient f	10000 N·s/m
-spring constant k	108979,9 N/m
Hydraulic cylinder:	
-piston section S	$7{,}5\cdot10^{-4}$ m^2
-stroke l	$13{,}7\cdot10^{-2}$ m
-pipes volume V_0	$0{,}39\cdot10^{-6}$ m^3
-leakage constant between chambers c_{12}	$2\cdot10^{-13}$ m^3/(Pa·s)
-leakage constant to exterior c_1	$1{,}68\cdot10^{-13}$ m^3/(Pa·s)
Pump parameters:	
- displacement D:	$0{,}169\cdot10^{-6}$ m^3/rad
- pump leakage constant c_2	$2\cdot10^{-13}$ m^3/(Pa·s)
Electric motor parameters	
-coil inductance L:	10^{-3} H
-coil resistance R:	0,35 Ω
-back-EMF constant k_e:	0,063 V·s/rad
-torque constant k_t:	0,0663 N·m/A
-momentum J:	$2{,}4\cdot10^{-5}$ kg·m^2
-friction coefficient B:	0,004 kg·m·s

For the numerical simulations the algorithm Dormand-Prince with variable step was used. The minimum step size was set at 10^{-6} s and the maximum step size was set at 10^{-4} s. The relative tolerance was set at 10^{-4}.

Different values of the step input were taken into account in order to determine the time response in each case. We neglected the dry friction force.

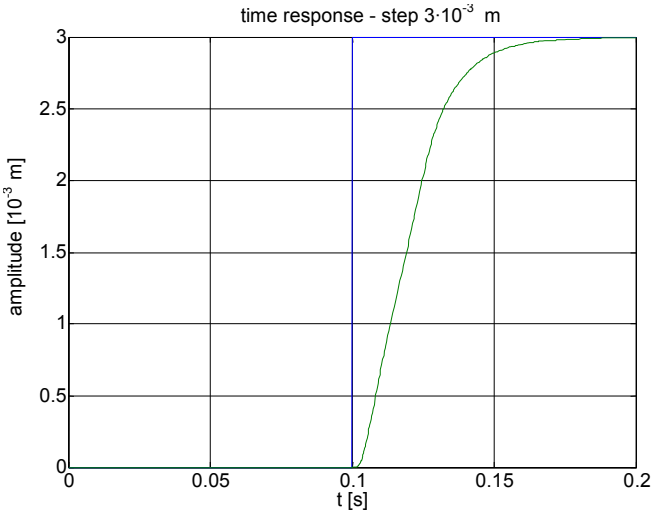

a

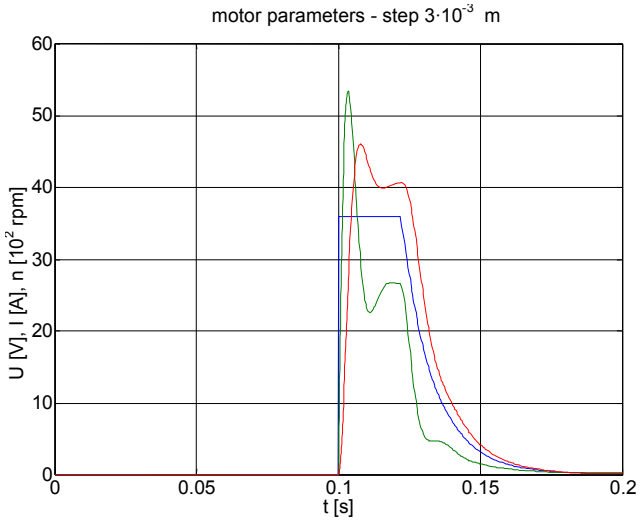

b

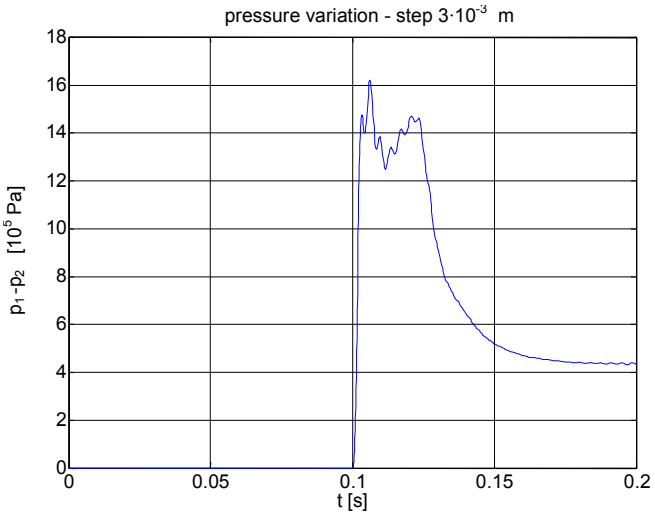

c

Fig. 5 System behaviour. P controller, step $3 \cdot 10^{-3}$ m

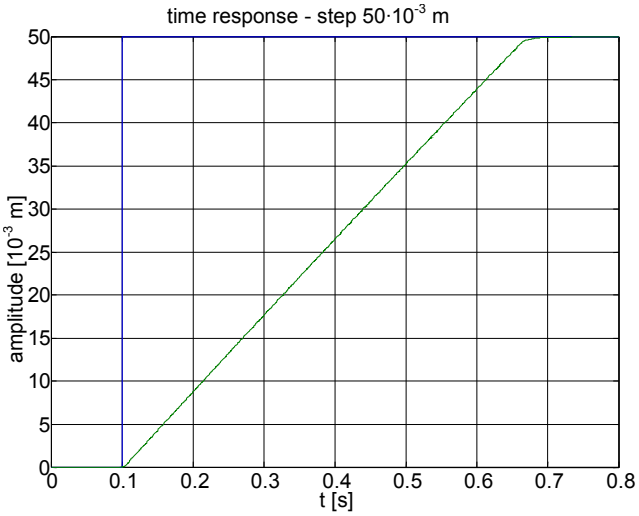

a

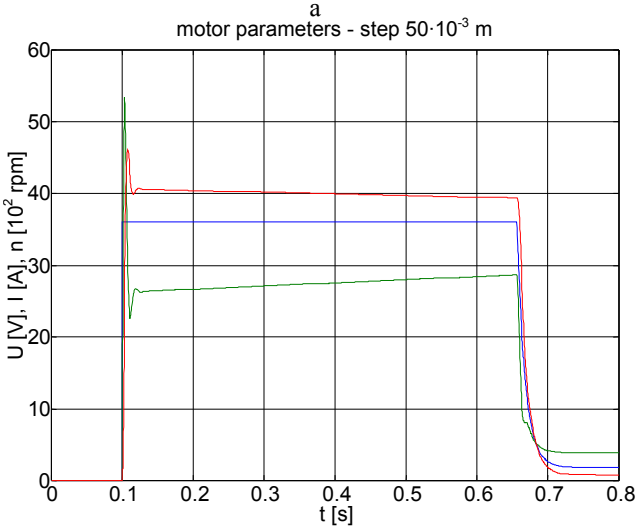

b

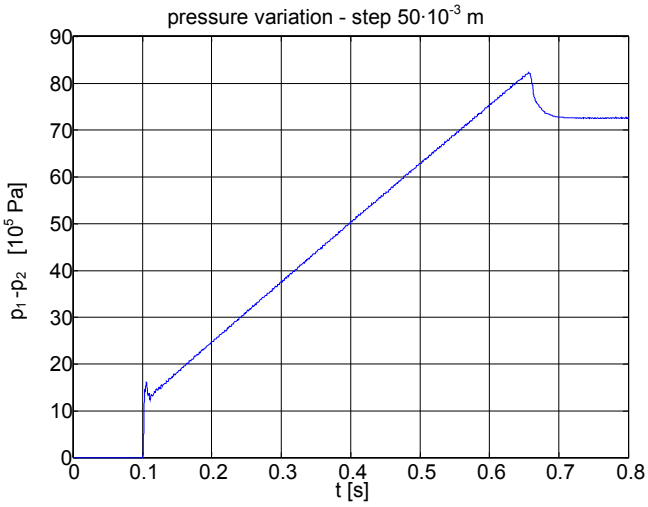

c

Fig. 6 System behaviour. P controller, step $50 \cdot 10^{-3}$ m

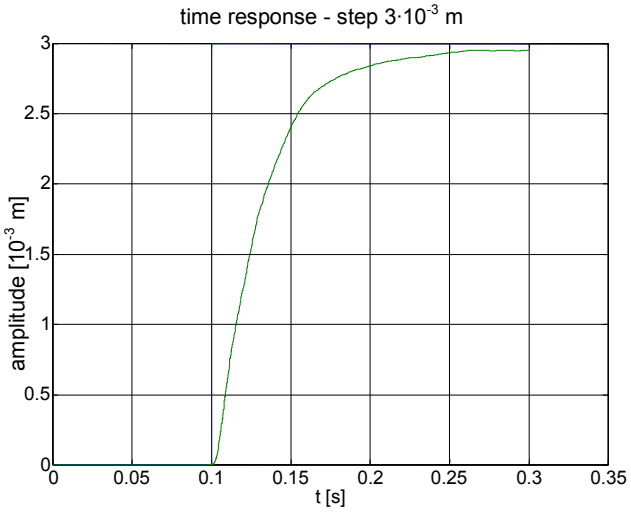

a

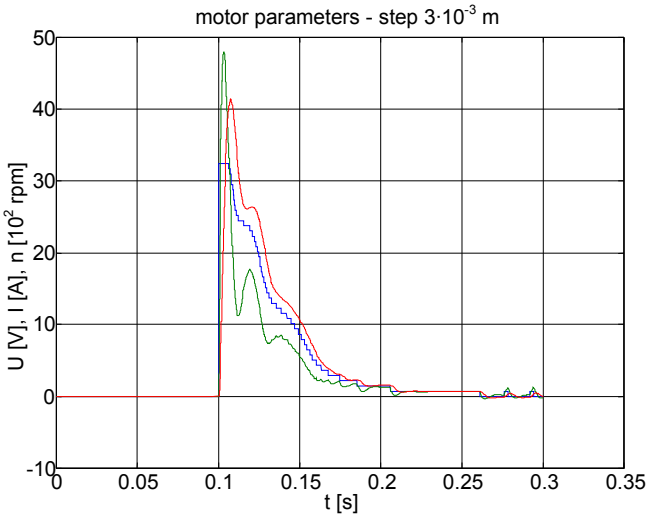

b

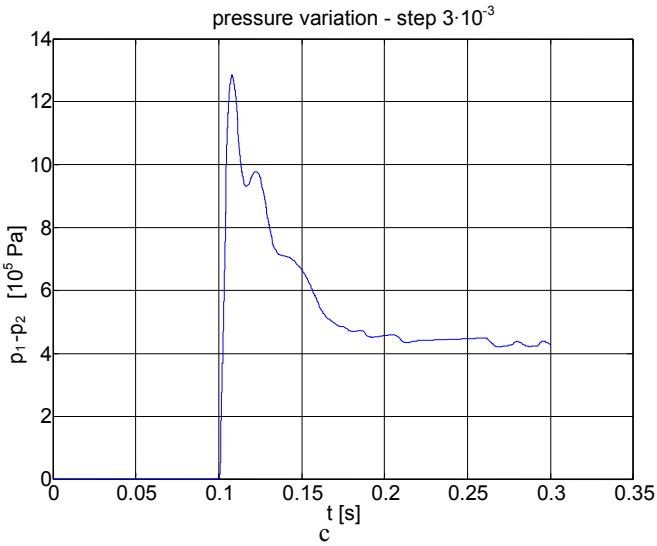

c

Fig. 7 System behaviour. Fuzzy controller, step $3 \cdot 10^{-3}$ m

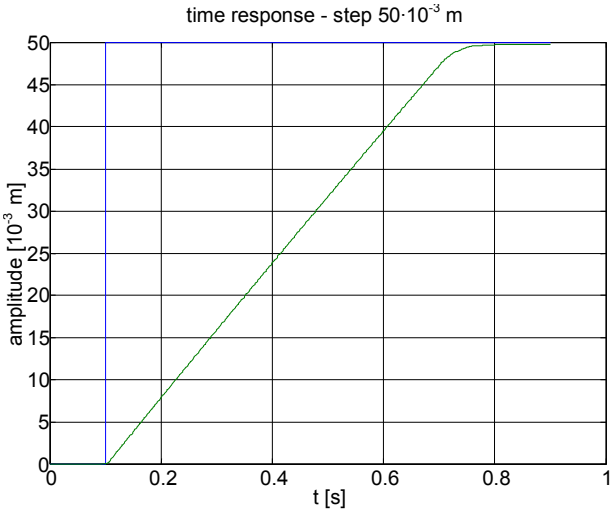

a

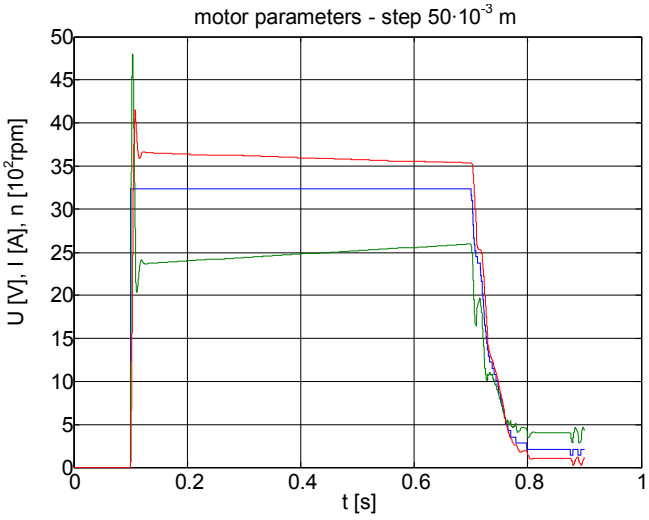

b

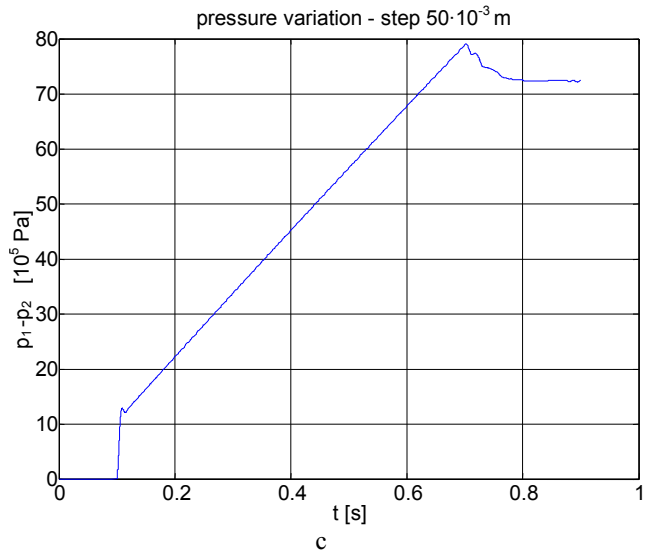

c

Fig. 8 System behaviour. Fuzzy controller, step $50 \cdot 10^{-3}$ m

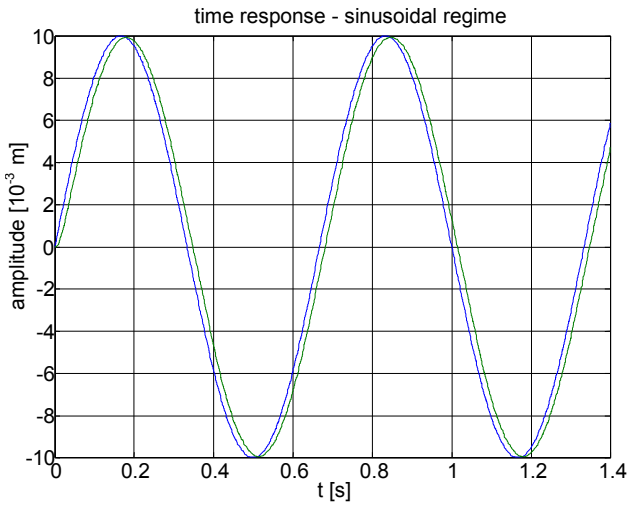

a

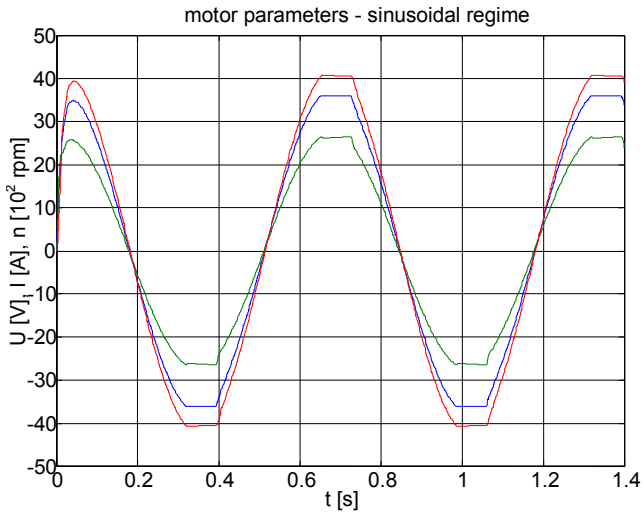

b

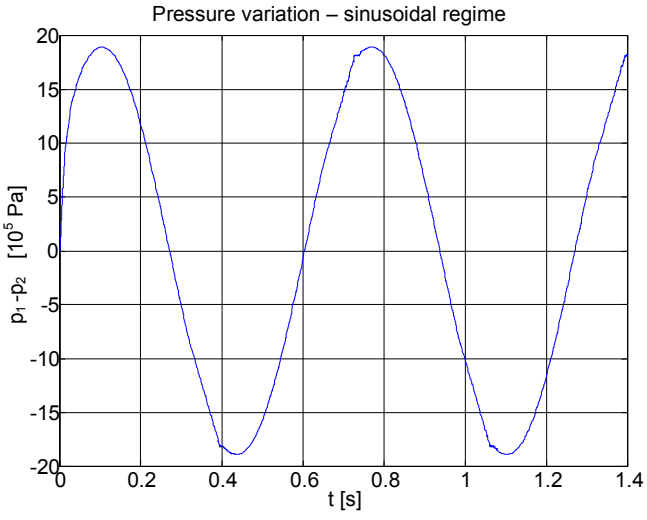

c

Fig. 9 – System behaviour – sinusoidal regime

V. Mathematical Model With Mass Flow Ratio

The numerical simulations presented before are realized considering a hydraulic cylinder with bilateral rod. In aviation there are not used these kind of cylinders due to the space necessary for the second rod who is not used.

Numerical simulations performed for mechano-hydraulic servo-actuators [5] proved that a mathematical model who take into account the liquid mass contained in the cylinder chambers, the leakage mass flow ratios, and the mass flow ratios conveyed by the pump, put in evidence more realistic some phenomena like the auto-oscillations with a frequency about 30 Hz.

Because we want to realize an electro-hydrostatic servo-actuator for aviation we will use in the future an unilateral rod cylinder. Taking into account the difference between the necessary flow ratios for the two cylinder chambers and the results mentioned before we will develop in the following a mathematical model with mass flow ratios for the servo-actuator studied in this paper.

We will supplement the scheme in fig. 4 with a hydro-accumulator and four valves, like in fig. 10.

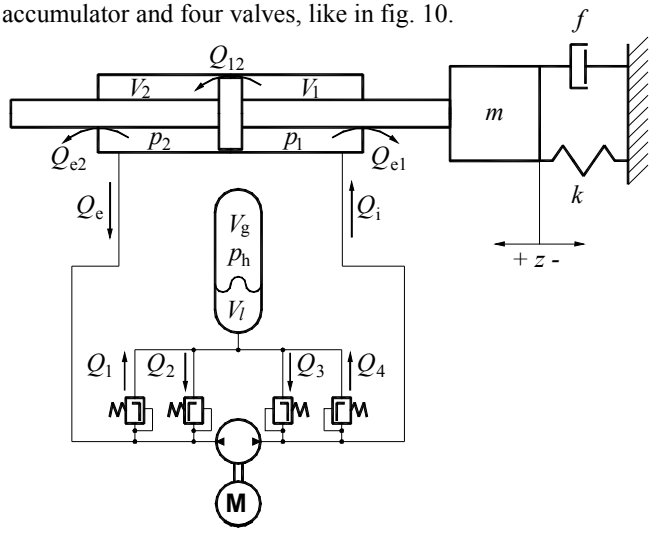

Fig. 10 Electro-hydrostatic actuator with hydro-accumulator and valves

The valves 1 and 4 are discharge valves which opens when the pressure in one chamber exceeds $230 \cdot 10^5$ Pa. Valves 2 and 3 are anti-cavitation valves which opens when de pressure drop under 10^5 Pa. By this way the hydro-accumulator restricts the pressure peaks at $230 \cdot 10^5$ Pa and feed the hydraulic circuit when a liquid deficit appears.

We will also take into account the leakage flow ratios of the pump like is shown in fig. 11.

In order to determine the pressure in the hydraulic cylinder chambers we will use the state equation of the liquid:

$$\rho = \rho_0 (1 + \beta \cdot p) \tag{16}$$

We will determine the liquid masses in each chamber and after that the chambers volumes.

From the density expression

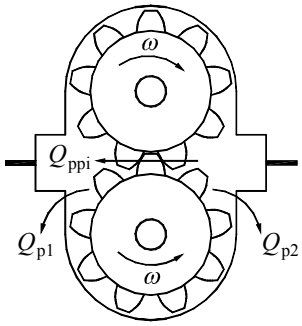

Fig. 11 Leakage flows of the pump

$$\rho = \frac{m}{V}, \tag{17}$$

results the pressure

$$p = \frac{1}{\beta} \cdot \left(\frac{m}{\rho_0 \cdot V} - 1 \right). \tag{18}$$

In (18) the chambers volumes are

$$V_1 = V_{10} + S \cdot z, \tag{19}$$

$$V_2 = V_{20} - S \cdot z. \tag{20}$$

Relations (19) and (20) were although used in (1) and (2).

In order to calculate the liquid mass in each chamber we will note Q_{tm} the mass flow ratio conveyed by the pump. This flow may be calculate using

$$Q_{tm} = \begin{cases} \rho_2 \cdot D \cdot \omega, & \omega > 0 \\ \rho_1 \cdot D \cdot \omega, & \omega < 0 \end{cases}. \tag{21}$$

After that, from the continuity equation results

$$Q_{tm} = Q_{em} - Q_{1m} + Q_{2m} + Q_{ppim} - Q_{p2m}, \tag{22}$$

$$Q_{tm} = Q_{im} + Q_{4m} - Q_{3m} + Q_{ppim} + Q_{p1m}. \tag{23}$$

From fig. 10 we obtain

$$m_1 = m_{10} + \int_0^t (Q_{im} - Q_{e1m} - Q_{12m}) \mathrm{d}t, \tag{24}$$

$$m_2 = m_{20} - \int_0^t (Q_{em} + Q_{e2m} - Q_{12m}) \mathrm{d}t. \tag{25}$$

In (24) and (25) Q_{im} and Q_{em} result from (22) and (23).

The external leakage of the pump may be calculate with

$$Q_{p1m} = \rho_1 \cdot Q_{p1} = \rho_1 \cdot c_2 \cdot p, \tag{26}$$

$$Q_{p2m} = \rho_2 \cdot Q_{p2} = \rho_2 \cdot c_2 \cdot p_2, \tag{27}$$

and the mass leakage between pump chambers

$$Q_{ppim} = \begin{cases} \rho_1 \cdot c_3 \cdot (p_1 - p_2), & p_1 \geq p_2 \\ \rho_2 \cdot c_3 \cdot (p_1 - p_2), & p_1 < p_2 \end{cases}. \tag{28}$$

For the mass leakage of the hydraulic cylinder we will use analog relations:

$$Q_{e1m} = \rho_1 \cdot c_1 \cdot p_1, \tag{29}$$

$$Q_{e2m} = \rho_2 \cdot c_1 \cdot p_2, \tag{30}$$

and for the leakage between cylinder chambers

$$Q_{12m} = \begin{cases} \rho_1 \cdot c_{12} \cdot (p_1 - p_2), & p_1 \geq p_2 \\ \rho_2 \cdot c_{12} \cdot (p_1 - p_2), & p_1 < p_2 \end{cases}. \tag{31}$$

Because the valves 1 and 4 are discharge valves, the mass flow ratio Q_{1m} and Q_{4m} are

$$Q_{1m} = \begin{cases} \rho_2 \cdot c_4 \cdot \sqrt{p_2 - p_h}, & p_2 > 230 \text{ bar} \\ 0, & p_2 \leq 230 \text{ bar} \end{cases}, \tag{32}$$

$$Q_{4m} = \begin{cases} \rho_1 \cdot c_4 \cdot \sqrt{p_1 - p_h}, & p_1 > 230 \text{ bar} \\ 0, & p_1 \leq 230 \text{ bar} \end{cases}. \tag{33}$$

The valves 2 and 3 are anti-cavitation valves so the mass flow ratio through it are

$$Q_{2m} = \begin{cases} \rho_h \cdot c_5 \cdot \sqrt{p_h - p_2}, & p_2 < 1 \text{ bar} \\ 0, & p_2 \geq 1 \text{ bar} \end{cases}, \tag{34}$$

$$Q_{3m} = \begin{cases} \rho_h \cdot c_5 \cdot \sqrt{p_h - p_1}, & p_1 < 1 \text{ bar} \\ 0, & p_1 \geq 1 \text{ bar} \end{cases}. \tag{35}$$

In order to determine the hydro-accumulator pressure we will suppose an isotherm gas evolution, so

$$p_h = \frac{p_{0h} \cdot V_{0g}}{V_g}. \tag{36}$$

The gas volume is

$$V_g = V_t - V_l, \tag{37}$$

where V_t is the total volume of the hydro-accumulator and V_l is the hydro-accumulator liquid volume.

The hydro-accumulator liquid volume is

$$V_l = \frac{m_l}{\rho_l} \tag{38}$$

For numerical integration we will use at each step the value of ρ_l from the previous step, calculated with (16).

The liquid mass in the hydro-accumulator is

$$m_l = m_{0l} + \int_0^t (Q_{1m} - Q_{2m} - Q_{3m} + Q_{4m})\mathrm{d}t \tag{39}$$

Using (36) – (39) and (16) we made a mathematical model for the hydro-accumulator in order to determine the pressure p_h which is used in (32) – (35).

VI. Numerical Simulations For The Mass Flow Ratio Model

For the numerical simulations in this case we used the same parameters we used before. Some parameters appeared supplementary:

- leakage constant between pump chambers c_3 — $3{,}3\cdot10^{-12}$ m^3/(Pa·s)
- flow constant of the discharge valve c_4 — $4{,}604\cdot10^{-8}$ m^3/(s·$\sqrt{Pa}$)
- flow constant of the anti-cavitation valve c_5 — $5{,}276\cdot10^{-8}$ m^3/(s·$\sqrt{Pa}$)
- total volume of the hydro-accumulator V_t — 10^{-3} m^3
- initial volume of the gas V_{0g} — $5\cdot10^{-4}$ m^3
- initial pressure of the gas p_{0g} — 10^7 Pa
- liquid density at zero pressure ρ_0 — 1050 kg/m^3

The initial masses of the liquid in the cylinder chambers were calculated using for the density the value corresponding a pressure of 10^6 Pa.

The numerical simulations were performed first for the mathematical model of the hydraulic subsystem and after that for the servo-actuator with P controller. Different cases were taken into account, from k=0 N/m which correspond to a flight speed of 0 km/h to k= 300000 N/m, an extreme value to verify the behaviour of the system when the check valves opens.

Due to the delay blocks used in the numerical scheme to avoid algebraic loops, it was necessary to use a step of time $2\cdot10^{-5}$ s. The integration method was Dormand-Prince with fixed step. The simulation time in this case was considerably larger that the cases considered before, but the simulation results are more realistic.

The results reflects the moments when the valves open and the stall phenomenon of the servo-actuator in the case of extreme value of k. In order to reach the opening pressure of the discharge valves, internal leakages of cylinder and pump were considered zero. Otherwise, the stall phenomenon appears but the servo-actuator do not reach that pressure.

Due to the internal and external leakage the anti-cavitation valve opens as we observe from the following figures.

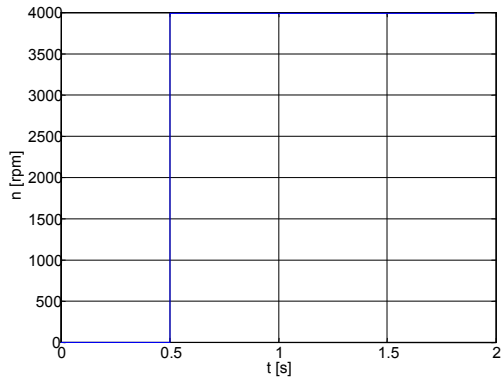

a

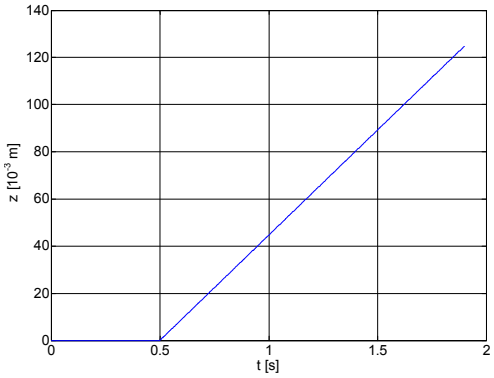

b

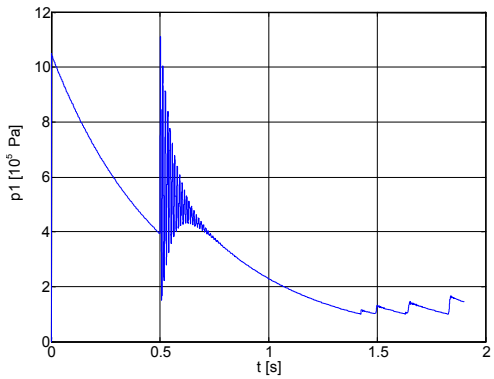

c

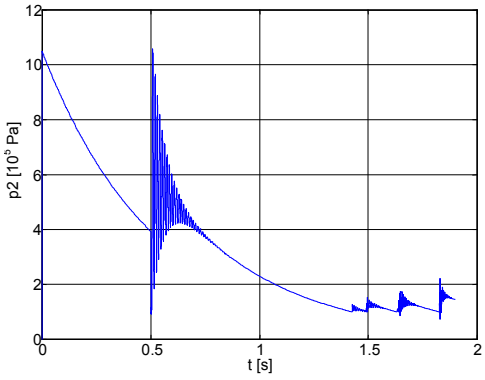

d

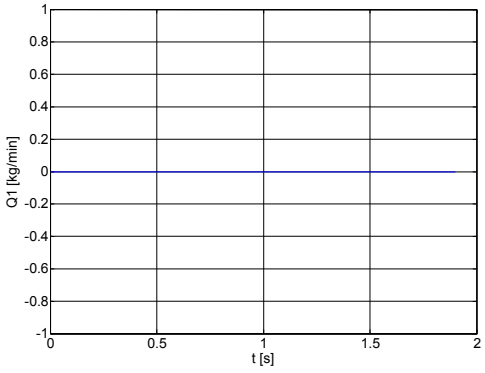

e

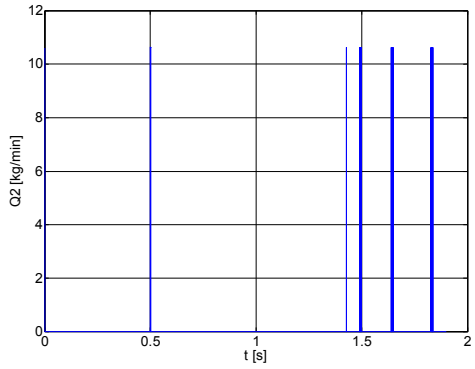

f

Fig. 12 Hydraulic subsystem behaviour at step of motor angular speed ($f = 0$, $k = 0$)

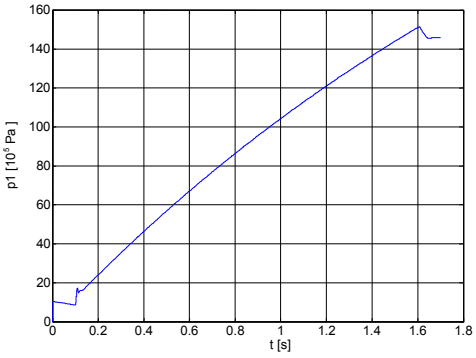

c

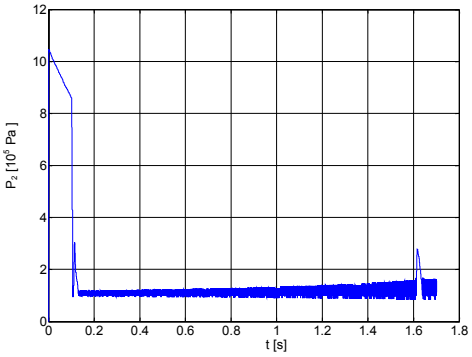

d

Fig. 13 Servo-actuator behaviour at step input. Parameters of simulation are those presented before

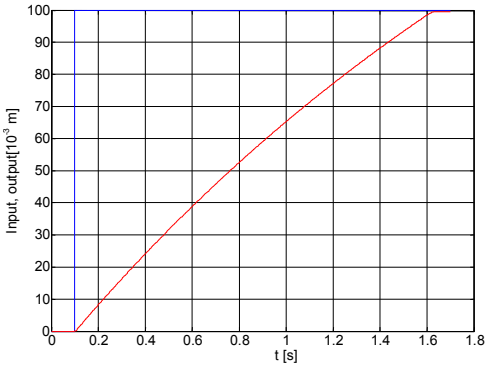

a

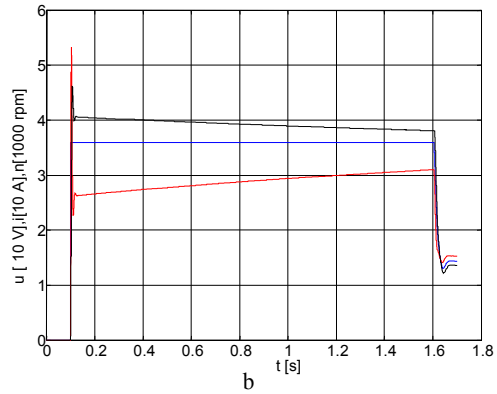

b

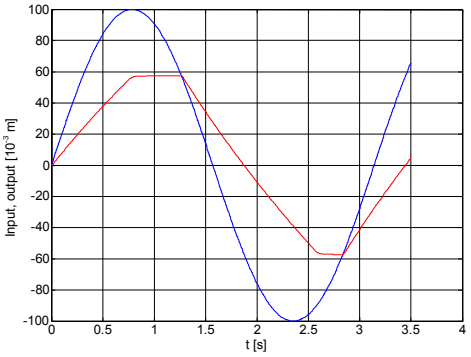

a

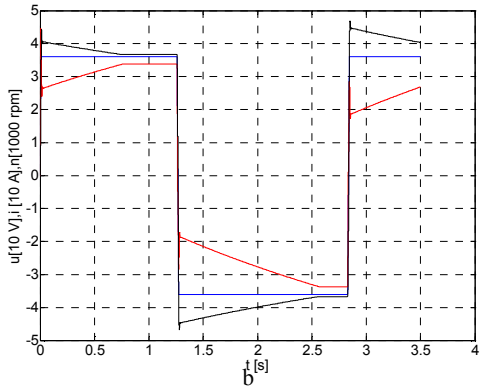

b

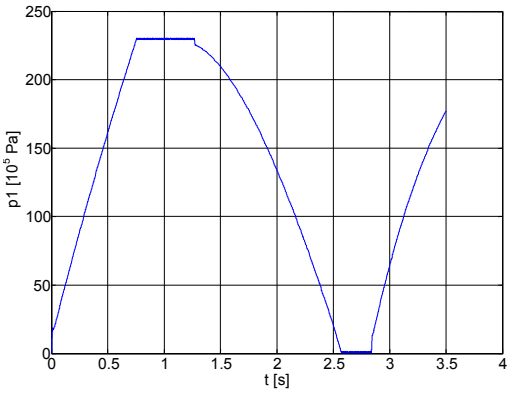

c

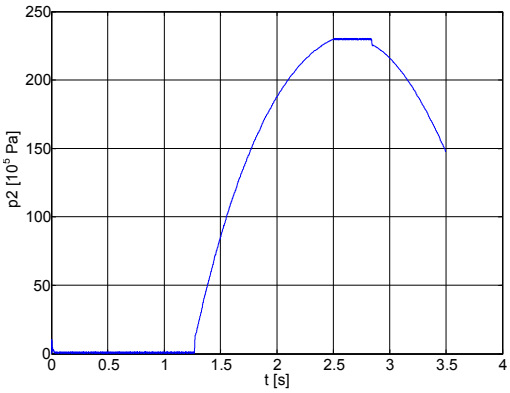

d

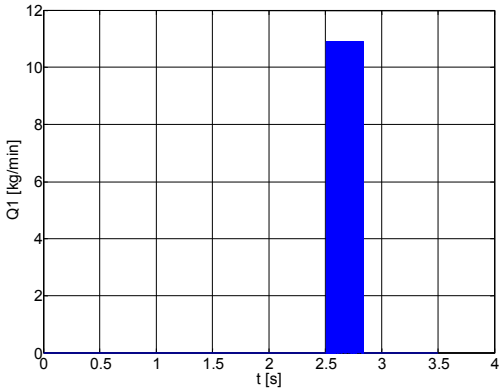

e

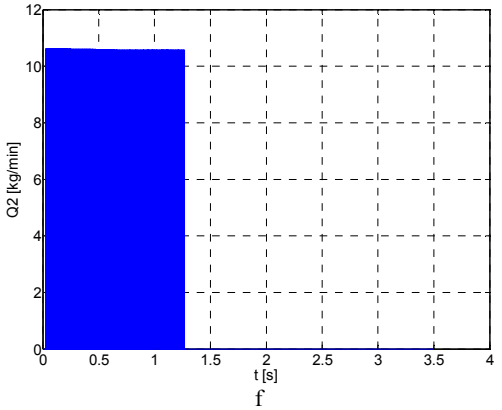

f

Fig.14 Servo-actuator behaviour. Sinusoidal regime, k =3·10^5 N/m, without leakage

VII. Conclusion

The results obtained from the numerical simulations reflect a good behaviour of the servo-actuator regarding the time response at step signal when a classical P controller is used. The time response parameters are in the limits imposed for the aircraft command surfaces actuators.

When a fuzzy controller is used, the servo-actuator is sluggish so it can be improved to obtain better results. One way to improve the fuzzy controller is to modify the membership functions in order to accelerate the servo-actuator movement.

For the servo-actuator presented in this paper the results obtained with the mass flow ratio model and the volume flow ratio model are very close when there are not reached the opening conditions for the valves. The leakage considered in the pump with the coefficient c_3 which in bigger than the other coefficients leads to a non linear variation of the output (see fig. 13. a and 8.a). Although when we linearised (1) and (2) we neglected the variations of the chambers volume in the left hand term, the results are close with the second model.

The mathematical model with mass flow ratios, although sluggish in simulations, offer a better image of the servo-actuator functioning. This model is not useful for the servo-actuator dimensioning, but it may be used to verify the dimensioning results. It may be useful although for the study of the electro-hydrostatic servo-actuator with unilateral rod cylinder. In this case the valves will be often opened, so the pressure in the hydro-accumulator and the flows through the valves will be very important.

Difficult problems in this actuator implementation will appear in the electric power distribution. This actuator needs high power invertors when it is used on big aircraft. Despite this, this type of servo-actuator it is expected to be the future in the aerodynamic surfaces actuation.

References

[1] I. Ursu, G. Tecuceanu, F. Ursu, A. Toader, "Nonlinear control synthesis for hydrostatic type flight controls electrohydraulic actuators." Conference Recent Advances in Aerospace Actuation Systems and Components, 13-15 iunie 2007, Toulouse, France;

[2] V. Pastrakuljic, "Design and modeling of a new electrohydraulic actuator". Ph.D. thesis at Mechanical engineering department of the Toronto University, 1995;

[3] S. Botten, C. Whitley, A. King, "Flight Control Actuation Technology for Next-Generation All-Electric Aircraft", Technology Review Journal – Millenium Issue – Fall/Winter 2000;

[4] R. Navarro, "Performance of an Electro-Hydrostatic Actuator on the F-18 Systems Research Aircraft", Research report. NASA Dryden Flight Research Center Edwards, California, october 1997;

[5] L. Dinca , "Numerical simulation of the aircraft hydro-pneumatic equipments " . Ph. D. thesis at University Politehnica Bucharest, 2005;

[6] D. Popescu, E. Bobasu, "Robust control design for an electro-hydraulic system using reduced order models". WSEAS transactions on systems, Issue 7, Volume 5, July 2006;

[7] O. Fan, J. Shackelton, T. Kalgonova, "Automation of electro-hydraulic routing design using hybrid artificially-intelligent techniques". WSEAS transactions on systems, Issue 7, Volume 5, July 2006;

[8] A.D. Henderson, J.E. Sargison, G.J. Walker, J. Haynes, "A numerical prediction of the hydrodynamic torque acting on a safety butterfly valve in hydro-electric power scheme". WSEAS transactions on fluid dynamics, Issue 3, Volume 3, July 2008